International Journal of Engineering and Technology Innovation, vol. 12, no. 4, 2022, pp. 336-346

Numerical Study of Vortex Flow in a Classifier with Coaxial Tubes

Vadim Zinurov[1], Vitaly Kharkov[2,*], Evgeny Pankratov[3], Andrey Dmitriev[1]

[1]Theoretical Foundations of Heat Engineering, Kazan Power Engineering University, Kazan, Russia

[2]Department of Food Production Equipment, National Research technological University, Kazan, Russia

[3]Department of Power and Heat Engineering, Northern (Arctic) Federal University, Arkhangelsk, Russia

Received 26 February 2022; received in revised form 06 May 2022; accepted 07 May 2022

DOI: https://doi.org/10.46604/ijeti.2022.9568

Abstract

Centrifugal air classifiers are one of the most used separation devices in particle technology. The study aims to obtain a detailed description of the bulk material classification mechanism in the developed centrifugal classifier. The classifier design and the mechanism of the stable vortex structure formation in the inter-tube space of the device are described. Velocities within and between the vortices are studied to identify regions with inverse flows, which serve as transport channels for particles. The computational fluid dynamics modeling results indicate three channels with negative or near-zero axial velocities: between the vortices, near the outer wall of the internal tube, and the inner wall of the external tube. The selectivity of the device decreases when transport channels are disrupted due to flow mixing, which is caused by the height shifting of the vortex centers.

Keywords: separation efficiency, tube classifier, vortex, velocity field

1. Introduction

Classification processes for solid mixtures are used in various energy, chemical, pharmaceutical, and other industries. The final properties of the products depend on the efficiency of the separation, especially when a calibrated powder is required [1]. The classification process is influenced by various factors, such as the two-phase flow, polydispersity, non-uniformity of the velocity field of the continuous phase and the local particle concentration fields, the rotation of particles in the flow, and others. Thus, the classification is a complicated and multivariable process [2-4].

There are three typical separation methods: mechanical, pneumatic (air), and hydraulic. In mechanical classifiers, the transport of material along the separating surface occurs because of the movement of particles on an inclined surface or (and) the periodic motion of the surface itself. In pneumatic classifiers, gas serves as the carrier medium for particles, forming a gas-dispersed flow (through-pass classifiers) or concentrated flow (fluidized bed classifiers), as well as an intermediate flow from a concentrated state to the gas-dispersed one. The carrier medium can remain stationary in individual air classifier designs. They operate at high temperatures and pressures, as well as with aggressive fluids. Hydraulic classifiers are based on the same principles as air devices, but use liquid as the carrier medium.

The most common and effective separation devices for solid dispersion systems are pneumatic classifiers, which can operate in a closed-air circuit; therefore, they do not generate dust and meet environmental requirements. According to Rumpf's work [5], there are gravitational and centrifugal separation zones in pneumatic classifiers; therefore, they are divided into gravity and centrifugal. Typical gravity pneumatic classifiers are chambers in which the air velocity is extremely low for

* Corresponding author. E-mail address: v.v.kharkov@gmail.com

Tel.: +79872679796

particle settling. When the airflow slows down and moves downwards, gravity captures large particles and ejects them from the air, but fine particles continue to flow with the airflow. Gravity separators are effective only for separating coarse particles larger than 50 μm. Moreover, they have high dimensions since gravitational acceleration is small, and the particles need a large space to be separated.

Using the centrifugal field to classify particles is the up-to-date separation method. Centrifugal pneumatic classifiers are more efficient because the centrifugal force acting on the particles can be thousands of times greater than the gravity force acting on the identical particles in the gravity classifier. The centrifugal air classification is the primary techno-economic method to separate solid particles of 3–100 μm in size. Therefore, interest in optimizing the process is important.

The authors have designed a pneumatic vortex classifier with coaxial tubes [6-7]. Distinctive features of the device are high selectivity with low-pressure losses, simplicity of the design regarding lack of moving mechanisms, low capital, and operating costs.

The work aims to obtain a detailed description of the classification mechanism of bulk materials in the developed centrifugal classifier. It is planned to numerically determine the local velocities of the vortex flow in the classifier's inter-tube space and evaluate the pressure losses. According to the results, negative axial velocities in certain regions of the inter-tube space indicate the existence of transport channels, i.e., circulation flows. Particles entering these regions are transported to the bunker. The distributions of axial velocities inside the vortex characterize the regularity of the vortex structure relative to its center by its height. The pressure drop of the developed classifiers is the lowest compared to other static centrifugal air classifiers. The analysis of the flow field is helpful to the design of the new classifier, which provides some guidance on the choice of experimental parameters.

2. Literature Review

Yoshida et al. [8] presented a meta-model of vertical air classification based on the stochastic process of particle separation. They found that the Lynch-Rao model was more flexible than the cumulative Weibull model. Fu et al. [9] have studied the performance of a centrifugal classifier at different heights, creating more favorable conditions for the sequential separation of fine particles. Both the velocity field and turbulence can affect the cut particle size and separation efficiency [10].

Computational fluid dynamics modeling (CFD) is a cost-effective and time-saving tool for studying particle classification for a long time. Sun et al. [11-13] have studied the flow field and performance of the horizontal turbo air classifier using the CFD method and response surface methodology (RSM). RSM was proven to be more suitable for simulating the air classifier than the k-ε model. The discrete phase model (DPM) can well predict the cut size of the classifier [14]. Liu et al. [15] have simulated the flow field of a turbo air classifier by Fluent package, changing the axial direction of airflow.

Yu et al. [16] numerically calculated the flow field distribution in a turbo air classifier with a volute profile. They found that the logarithmic spiral volute has a good effect on guiding the airflow and can form a well-distributed flow field in the classifier, improving the classification efficiency. Similarly, Huang et al. [17] investigated the influence of the blade shape of the turbo air classifier on the flow field and classification precision. The results demonstrated that the positively bowed guide blade improves the classification performance and reduces particle cut size. Recently, Sun et al. [18] have studied the effect of fully inserted vortex finders of the centrifugal air device on particle classifying performance. The results indicate that the slotted vortex finder can reduce the influence of short circuit flow on coarse particles.

Betz et al. [19] have studied a classifier without and with flow baffles using DPM. The influence of baffles inside the device was estimated at the flow profile, pressure loss, and classification efficiency for different geometries under two operating conditions. Petit et al. [20] have modeled a classification mechanism inside the inclined plane classifier. The authors

computed particle trajectories in the classifier using a Lagrangian discrete phase modeling approach. Barimani et al. [21] used DPM to track particles in the airflow of a high-speed centrifugal classifier. The developed model allows calculating particulate concentration contours in the classifier. The authors concluded that fine particles strictly follow airflow.

Altun and Benzer [22] have developed a mathematical model for high-efficiency air classifiers by applying the efficiency curve approach. According to the research, the sharpness depends on the process capacity and classification chamber diameter. The modification of the separator by the attachment of the cylinder to the center of the centrifugal separator is expected to prevent the particles in the slurry from passing through the central axis of the centrifugal separator [23].

Feng et al. [24] have investigated the flow field in classifiers with different bottom incoming flow inlets using the particle image velocimetry technique. It was found that the separation efficiency of the device with the non-swirling inlet was lower than that with the swirling inlet, and that the efficiency monotonically increased with a rise in the impeller rotational speed.

From the literature survey, it is clear that evaluating the efficiency of the air classifiers is related to the particle classification mechanism, which is determined by the velocity field within the device. In particular, based on the velocity field in the various regions of the cyclonic classifier, Sun et al. [25] found that negative axial velocities in certain regions of the device increased the efficiency of particle classification. Thus, the novelty of this study is to describe a flow pattern in a classifier with coaxial tubes, where a stable vortex structure in the inter-tube space forms, which leads to increasing the efficiency of separation.

3. Objects and Methods

Fig. 1 represents the developed classifier, including internal and external cylindrical tubes. A perforated plate provides the fixation of the tubes and holes with a specified pitch made to discharge purified gas through connected hoses (not indicated here). In addition, these holes in the plate support the stable vortex structure in the inter-tube space of the device. The lower part of the internal tube has rectangular slots arranged uniformly over the cylindrical surface. Moreover, the slots are located precisely midway between every two holes in the plate. This technical solution ensures a uniform flow distribution across the classifier's inter-tube space and the formation of stable vortices. A conical hopper, mounted on the bottom of the inner tube, has a hole to exclude the clogging of the internal tube by coarse particles, which settle from the dirty flow. The conical shape of the hopper enables the formation of smoother inverse flows compared to other forms. Inverse flows in the inter-tube space are undesirable because they cause destructive action on the stable vortex structure.

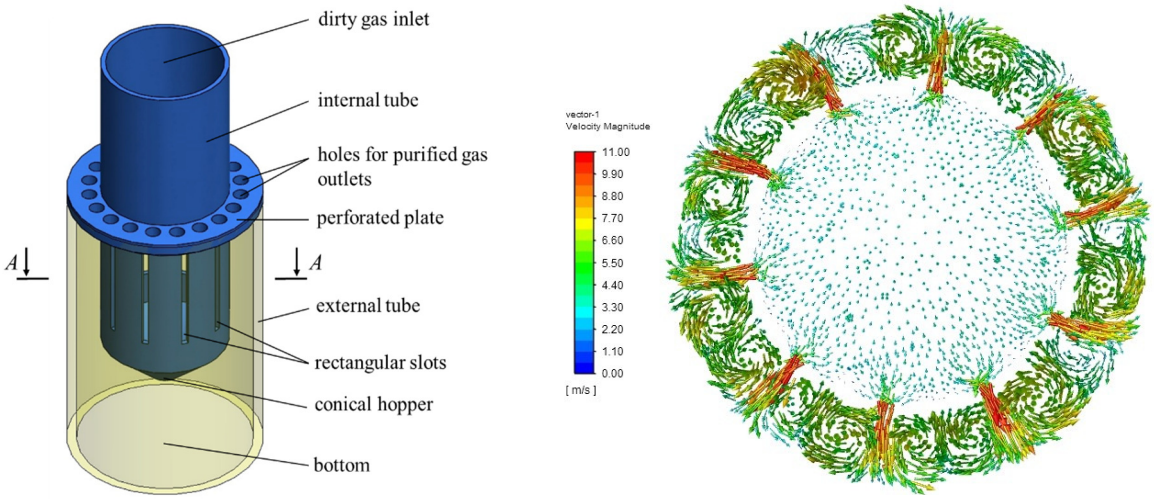

(a) 3D model (b) A-A cross-section (vortex structure simulation)

Fig. 1 Classifier with coaxial tubes

The classifier works as follows. The dirty flow enters the device via an inlet, and then flows down the internal tube. Then, the trajectory of the gas flow rapidly changes. When the gas reaches the slots, its direction changes to perpendicular. Therefore, the gas flow moves uniformly in an asymmetric direction on the rectangular slots. When the gas with particles passes through the slots, after each slot, the flow is divided into two equal vortices, rotated opposite to each other. And these vortices move up to the holes. Thus, the stable vortex structure forms in the inter-tube space. The vortex flow produces centrifugal forces that discard particles from the gas flow to the wall of the external tube. The separated particles fall to the bottom of the device, which is connected to the collector (not indicated here). Part of the gas flow with particles passing through the hole in the hopper is divided into several equal parts in the axially symmetrical direction and moves into the inter-tube space. Furthermore, when the gas flow changes by 180º, the largest particles fall out of the flow by inertia and into the bunker. Of course, the flow of upward gas from the hopper partially influences the structure of vortices in inter-tube space. The gas flow moves up to the upper part of the device, and passes through a plate with holes, which also acts as an extra separation element, ejecting particles from the gas.

Numerical simulations are performed on the developed three-dimensional classifier model using Ansys FLUENT. The geometric parameters of the 3D model are as follows. The internal tube has sizes: an outer diameter of 65.6 mm, a wall thickness of 2.5 mm, and a height of 190 mm. The external tube has sizes: an inner diameter of 95 mm, a wall thickness of 5 mm, and a height of 160 mm. The distance between the conical hopper and the bottom of the device is 50 mm. The perforated plate has 20 holes with a diameter of 8 mm. The conical hopper has a height of 22 mm with a 16 mm hole. The number of the rectangular slots is ten, with a height of 60 mm and a width of 3.5 mm. The condition of particles sticking is set as they contacted the bottom's surface.

Figs. 2(a)-(c) show the stages of a flow region formation based on the 3D solid model of the developed classifier. Since the model is axially symmetric, a 1/10 sector of the volume of the flow region is selected (Fig. 2(b)) under the condition that two vortices occur in the inter-tube space. This condition is determined by the mutual support of the vortices at contact points, where the vectors of local velocities are co-directed. The boundary of each sector on both sides is a transverse line, cutting the region of the rectangular slot in half.

Fourteen planes with a pitch of 10 mm (Fig. 3(a)) are generated in the flow region to find the distributions of the axial and radial velocities in a single vortex according to the height of the classifier. A diametrical line with a set of points is defined on each plane in the region of the specific vortex to construct dependencies for the axial W_z and radial W_φ velocities. The local coordinates on the diametral line are reduced to the dimensionless parameter of $2r/d_v$, where r is the calculated radius of the vortex, and d_v is the vortex diameter equals 12.2 mm. Therefore, the center of the vortex corresponds to 0 and the extreme points correspond to –1 and +1 (Fig. 3(b)). Also of particular interest is the study of the axial velocities of gas between vortices $W_{z.md}$, as they may form the inverse flows, working as transport channels for particles. Therefore, an additional line is drawn between the vortices, similar to the diametral line in the single vortex, to study $W_{z.md}$ (Fig. 3(b)).

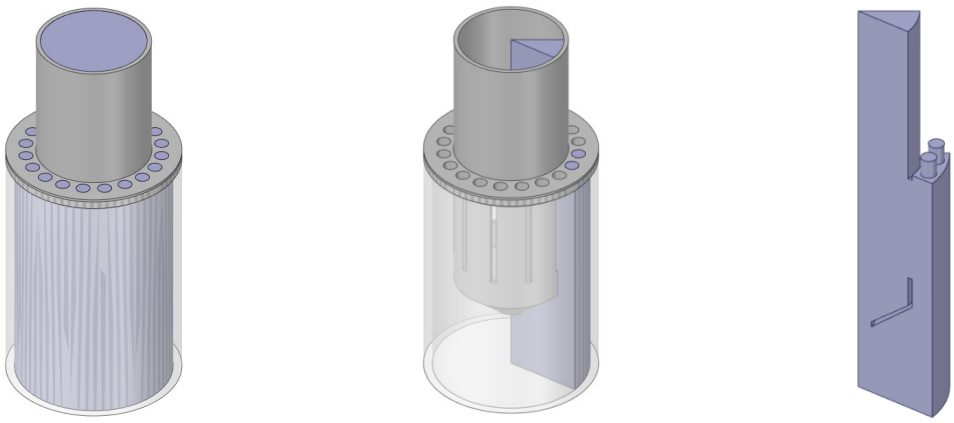

(a) Formation of the flow region (b) Selection of 1/10 volume of the flow region (c) Flow region geometry

Fig. 2 Preparation of the 3D model of the classifier with coaxial pipes for sector modeling

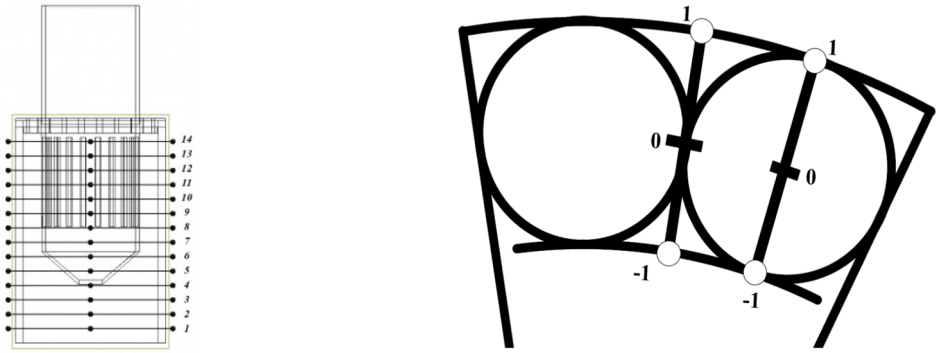

(a) Planes (b) Computational lines in the sector

Fig. 3 Visualization of planes and computational lines in the classifier for the study of axial and radial velocities

The axial and radial velocity distributions are given dimensionless by their ratio to the velocity in the rectangular slot W_{sl}, which is calculated from the continuity equation for fluid flow as the following:

$$w_{sl} = \frac{\pi W d_{in}^2}{40 b_{sl} h_{sl}} \tag{1}$$

where W is the gas velocity at the inlet of the classifier, m/s; d_{in} is the inner diameter of the internal cylindrical pipe, m; b_{sl} is the width of the rectangular slots, m; h_{sl} is the height of the rectangular slots, m.

During the calculations, the inlet velocity of the gas flow W changes from 1 to 8 m/s. These parameters are constant: gas density – 1.205 kg/m^3, the dynamic viscosity of gas – 15.1 × 10^{-6} Pa, pressure at the classifier outlet – 10^5 Pa. A nonstationary solver is used in the numerical experiment. Velocity fields are considered from 0.01 to 0.10 s. Before setting the boundary conditions, the flow region is divided into 1,086,732 cells. For the ease of data analysis, all lines are divided into two categories defining the height of the planes in the classifier visualized in Fig. 2(a):

(1) Red lines with h_{sw} ranging from 10 to 80 mm characterize the velocity field below the rectangular slots at the bottom of the classifier;

(2) Blue lines with h_{sw} ranging from 90 to 140 mm describe the velocity field at the level of the rectangular slots.

4. Results and Discussion

The results of the nonstationary numerical simulations show that the response time to the quasi-steady flow is about 0.1 s. The dimensionless axial velocities in the spaces between the vortices and near the diametrical lines have negative values at some heights, proving the existence of transport channels. If particles enter these spaces, they are swept away by the gas in the opposite direction from the outlet holes and settle in the classifier bunker. However, at some heights, depending on the initial velocity of the gas flow, the dimensionless axial velocities only have positive values both between the vortices and in the vortices themselves, showing the absence of transport channels. Otherwise, when the particles reach a certain height in the apparatus, they leave the classifier through outlets with high probability, except when particles clog in or stick to irregularities in the inner walls of the classifier.

In most cases, negative dimensionless axial velocities between vortices can exist in all ranges of $2r/d_v$. In contrast, negative dimensionless axial velocities in the space of the vortex diametrical lines can only exist in the range $2r/d_v$ from -1.0 to -0.3 and from 0.7 to 1.0. The spread in negative values of the dimensionless axial velocities in the space between the vortices can be explained by the geometrical features of the classifier and the physics of the vortex motion. Particularly, vortices form with a specific diameter, depending on the size of the internal and external tubes and the size of the rectangular slots and the holes in the plate, which provides a more stable vortex structure in height. Ultimately, the vortices concentrate most of the gas that enters the classifier, and the gas that moves between the vortices can pass into a vortex flow, i.e., a low-pressure zone.

In some cases, as shown in Figs. 4(a)-(b), dimensionless axial velocity in the space between the vortices gradually shifts from negative and about zero values to positive in the length of the computational line in the sector. This phenomenon is related to the increasing in-feeding of the main flow in the inter-tube space through the rectangular slots, as they are located almost at the full height of the part of the internal tube inserted in the external tube. Furthermore, during rotation, the vortices can move some small distance from the center of the axis, which is sufficient to generate additional turbulence in the space between the vortices.

Predominantly, all negative values of dimensionless axial velocities in the vortex's space diametrical line are fixed close to the tube surfaces: the outer wall of the internal tube and the inner wall of the external tube, i.e., there may be an impact of the boundary layer. Note that the negative values of the dimensionless axial velocities are more significant in the space of the inner wall of the external tube than in the space of the outer wall of the internal tube. This fact is caused by an influx of air from the rectangular slots that partially or entirely destroy the boundary layer (Figs. 5(a)-(c)).

The dimensionless axial velocity between the vortices $W_{z.md}/W_{sl}$ is not over 0.8 at the inlet gas velocity of 1–8 m/s at 0.1 s (Fig. 4). The dimensionless axial velocity near the diametrical line of the vortex W_z/W_{sl} is less than 1.8, 1.3, and 1.3 at the gas inlet velocities of 1, 5, and 8 m/s, respectively, at 0.1 s (Fig. 5). Comparative analysis shows that the velocity inside the vortices is, on average, 1.9 times higher than that in the space between them.

The lines of the dimensionless radial velocities in the space of the diametrical lines of the vortex W_φ/W_{sl} are asymmetrical to their center, where $2r/d_v$ is 0. An important feature is that the vortex center ($2r/d_v = 0$) is often shifted by a certain distance, which is a reason for changing the axial velocities between vortices, thus disrupting the trajectories of particles in transport channels (Fig. 6). At the maximum deviation, if all 14 planes are considered (Figs. 6(a)-(c)), the center of the vortex along the abscissa and the ordinate (in absolute magnitude) is shifted by 0.6 and 0.24 (at W = 1 m/s), 0.1, and 0.14 (at W = 5 m/s), 0.16, and 0.09 (at W = 8 m/s), respectively. At lower velocities, the center of displacement of the vortex is expressed more strongly.

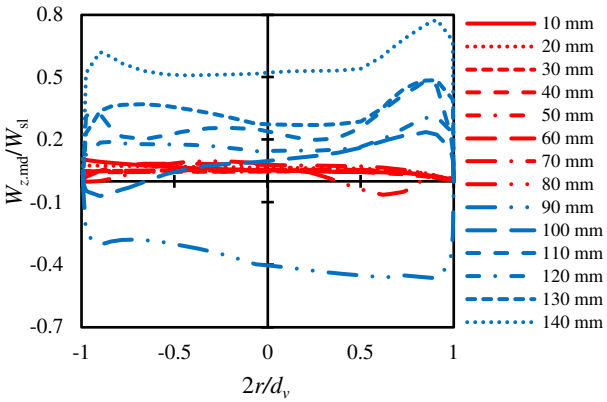

(a) Inlet velocity of the gas flow: 1 m/s (at the time of 0.1 s)

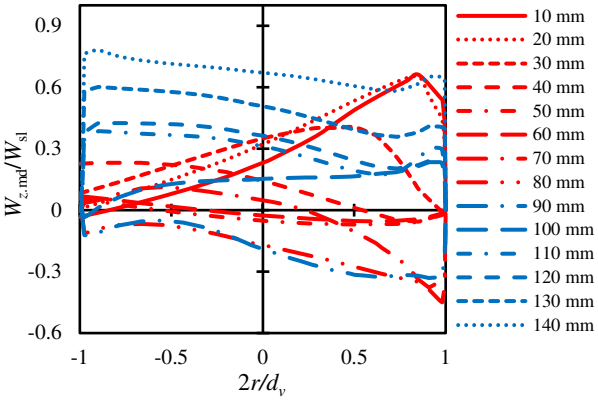

(b) Inlet velocity of the gas flow: 5 m/s (at the time of 0.1 s)

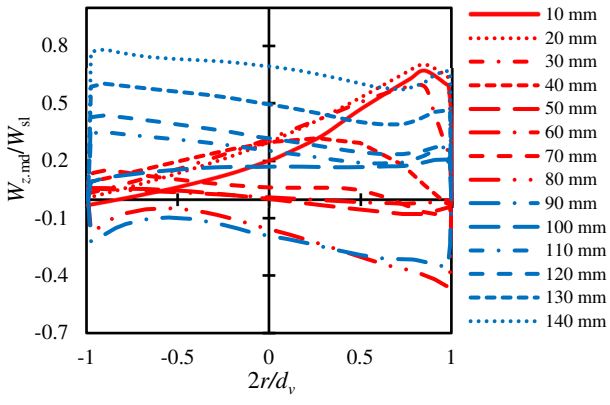

(c) Inlet velocity of the gas flow: 8 m/s (at the time of 0.1 s)

Fig. 4 Dimensionless axial velocity between the vortices at the dimensionless local points for different heights of the vortices from the bottom h_{sw}, mm

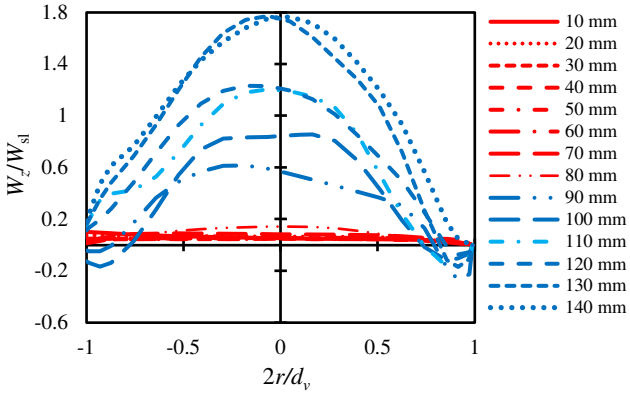

(a) Inlet velocity of the gas flow: 1 m/s (at the time of 0.1 s)

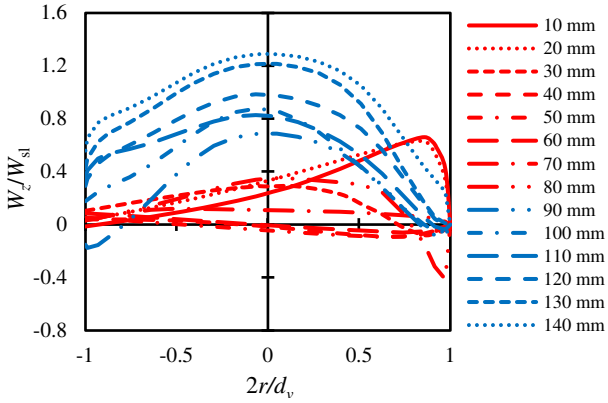

(b) Inlet velocity of the gas flow: 5 m/s (at the time of 0.1 s)

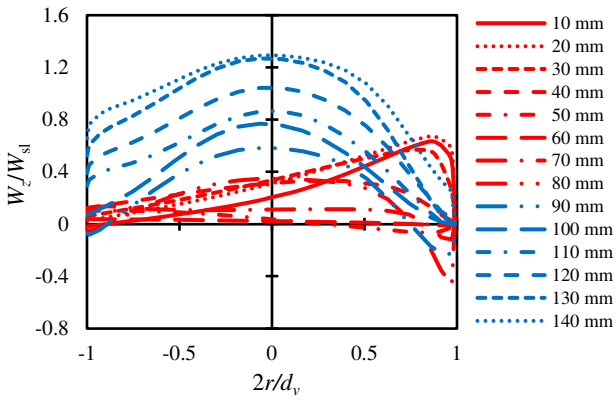

(c) Inlet velocity of the gas flow: 8 m/s (at the time of 0.1 s)

Fig. 5 Dimensionless axial velocity in the space of the vortex diametrical lines at the dimensionless local points for different heights of the vortices from the bottom h_{sw}, mm

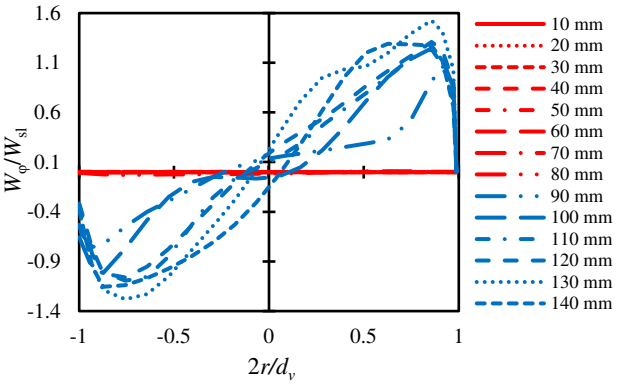

(a) Inlet velocity of the gas flow: 1 m/s (at the time of 0.1 s)

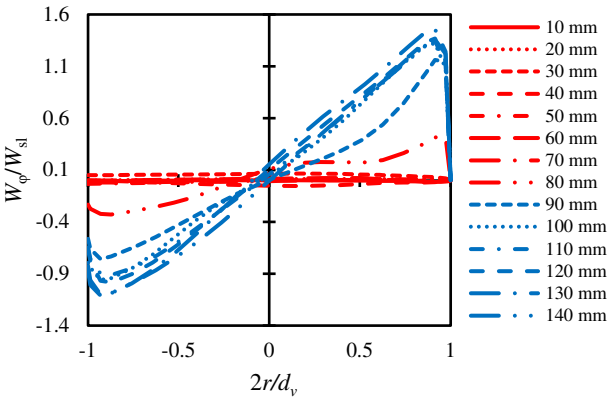

(b) Inlet velocity of the gas flow: 5 m/s (at the time of 0.1 s)

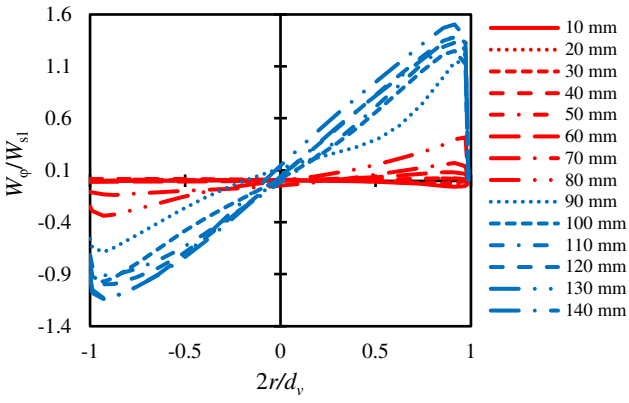

(c) Inlet velocity of the gas flow: 8 m/s (at the time of 0.1 s)

Fig. 6 Dimensionless radial velocity in the space of the vortex diametrical lines at the dimensionless local points for different heights of the vortices from the bottom h_{sw}, mm

Fig. 7 shows the relationship between the separation efficiency of the device with coaxial tubes versus the particle size at different gas velocities. The particles of 5–40 μm are of particular interest, since over one region with peaks within this size range can occur for each inlet gas velocity. Thus, by varying the inlet velocity of the gas flow, it is possible to separate solid particles of different critical sizes. The increased selectivity can be achieved by implementing multiple stages, i.e., sequentially installed classifiers. For example, at the inlet gas velocity of 1 m/s, the average separation efficiency for solid particles with sizes from 5 to 100 μm is 33.9%, and no peak regions. For particles less than 20 μm, separation efficiency is less than 20%.

At an inlet gas velocity of 2 m/s, there are two regions where the efficiency increases sharply (regions with peaks), corresponding to the particle range of 10–30 and 30–40 μm. The maximum efficiency for the first peak is 51.6%, and for the second – 31.1%. For the extremes of the first peak region, which correspond to particles of 10 and 30 μm in size, the classifier's efficiency is 5.6 and 18.7%, respectively. For the second region with particle sizes of 30 and 40 μm, the efficiency is 18.7 and 31.1%. When the inlet gas velocity is 5 m/s, there is one region with a peak corresponding to a particle range from 5 to 30 μm. The efficiency of this peak is 20.7% for 15 μm particles. At the region's boundaries, with a peak of 5 and 20 μm, the efficiency is 2.7 and 16.8%, respectively. At the inlet gas velocity of 8 m/s, there is one region with a peak. The boundaries are 5 and 20 μm with a peak at a particle size of 15 μm. The classifier's efficiency at 5, 20, and 15 μm is 4.1, 20.5, and 26.8%, respectively (Fig. 7).

The power relationship of pressure loss in the developed classifier with coaxial tubes is determined as the following:

$$\Delta p = 8.6W^{2.1} \tag{2}$$

The pressure loss in the developed classifier is not over 700 Pa at a gas velocity of up to 8 m/s (Fig. 8). Table 1 shows a comparison of pressure drops for different air classifiers working under the influence of centrifugal force. Dynamic air classifiers have the minimal pressure losses, but the developed classifier with coaxial tubes is the best choice among static separators because of the lowest pressure drop.

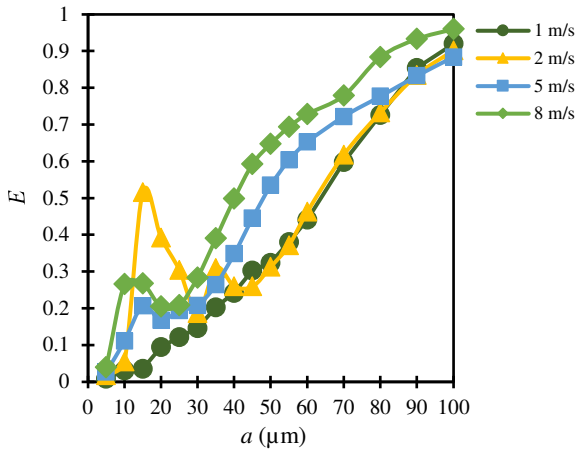

Fig. 7 Separation efficiency versus particle size at different inlet gas velocities *W*, m/s

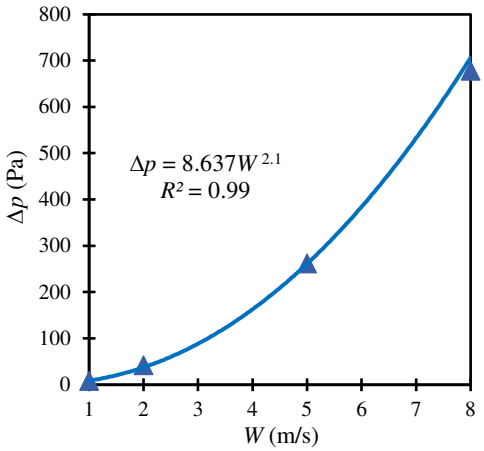

Fig. 8 Pressure drop of the classifier with coaxial tubes

Table 1 Pressure drop of different air classifiers

Name	Type	Maximal pressure drop (Pa)	Reference
Centrifugal air classifier (helix)	Static	900	[13]
Centrifugal air classifier with blades	Static	2000	[19]
Middle-inlet cyclone classifier	Static	2000	[25]
Separators (type A/type B)	Dynamic	958.8/1405.4	[26]
Cyclone separator	Static	2000	[27]
Rotor classifier	Dynamic	300	[28]
Cyclonic classifier	Static	1300	[29]
Classifier with coaxial tubes	Static	700	This study

Thus, the performed study shows that the developed design of the device provides a structured flow with multiple vortices in the inter-tube space and regions with negative or about zero velocities (transport channels). The rotation of many small vortices produces centrifugal forces that separate fine particles from the gas flow with high efficiency. This separation involves two mechanisms. First, the particles, entering spaces between vortices or near the inner wall of the external tube at a certain height, are carried away by a downward flow to the bottom collector. Second, the particles are captured by an upward flow and swept away by the gas flow.

An analysis of the flow field shows that the particle separation in the device is significantly determined by the inlet gas velocity, since it describes the oscillation of the vortices. Flow mixing occurs in the spaces between the vortices and near the outer wall of the internal tube and the inner wall of the external tube, which adversely affects the particle separation. In particular, when transport channels are disrupted and selectivity is reduced. As the inlet gas velocity increases, the vortex oscillation decreases. This is proved by the calculation time for the quasi-steady flow at different inlet gas velocities: at higher velocities of 5 and 8 m/s, the values of the parameters under study at 0.05 and 0.1 c are almost identical.

5. Conclusions

The vortex flow field in the developed classifier with coaxial tubes is numerically studied. The main conclusions may be summarized as follows:

(1) Separation of particles is performed through transport channels – spaces with negative or near-zero axial velocities. Three channels are identified: between the vortices, near the outer wall of the internal tube, and near the inner wall of the external tube.

(2) The negative dimensionless axial velocities in the vortex's space diametrical line exist only in the range $2r/d_v$ from -1 to -0.3 and from 0.7 to 1.0 (areas near the outer wall of the internal tube and the inner wall of the external tube).

(3) Velocity in vortices is, on average, 1.9 times higher than in space between vortices.

(4) The selectivity of the classifier decreases when transport channels are disrupted because of the mixing of the flow in these spaces. The flow mixing in the transport channels is caused by the height shifting of the vortex centers.

(5) The visualization of dimensionless radial velocity fields in the vortex diametrical lines detects the breakdown of vortices in the lower part of the classifier. Typically, the decay of the vortices occurs at heights of 80–90 mm.

(6) The analysis of the separation efficiency of the device with coaxial tubes shows more than one region with peaks for inlet gas velocities: 2, 5, and 8 m/s. In particular, at the inlet gas velocity of 2 m/s, there are two regions where the efficiency increases sharply (areas with peaks), corresponding to particle size ranges of 10 to 30 and 30 to 40 μm, one region with a peak for particles of 5 to 30 μm at 5 m/s, and one area with a peak for particles of 5 to 20 μm at 8 m/s.

(7) The pressure loss in the classifier is not over 700 Pa at a gas velocity of up to 8 m/s.

Acknowledgments

The reported study was funded by the grant of the President of Russia (№ MK-2710.2021.4).

Conflicts of Interest

The authors declare no conflicts of interest.

References

[1] K. Riener, et al., "Influence of Particle Size Distribution and Morphology on the Properties of the Powder Feedstock as Well as of AlSi10Mg Parts Produced by Laser Powder Bed Fusion (LPBF)," Additive Manufacturing, vol. 34, Article no. 101286, August 2020.

[2] E. Ortega-Rivas, Unit Operations of Particulate Solids: Theory and Practice, New York: CRC Press, 2017.

[3] V. Zinurov, et al., "Design of High-Efficiency Device for Gas Cleaning from Fine Solid Particles," 6th International Conference on Industrial Engineering, pp. 378-385, May 2021.

[4] I. N. Madyshev, et al., "Pressure Drop and Particle Collection Efficiency of Multivortex Separator," IOP Conference Series: Earth and Environmental Science, vol. 988, no. 4, Article no. 042069, February 2022.

[5] H. Rumpf, Particle Technology, London: Chapman and Hall, 1990.

[6] V. E. Zinurov, et al., "Classification of Bulk Material from the Gas Flow in a Device with Coaxially Arranged Pipes," E3S Web of Conferences, vol. 193, Article no. 01056, October 2020.

[7] V. E. Zinurov, et al., "The Gas Flow Dynamics in a Separator with Coaxially Arranged Pipes," MATEC Web of Conferences, vol. 329, Article no. 03035, November 2020.

[8] T. Yoshida, et al., "Meta-Model of Vertical Air Classification: A Unified Understanding of Different Separation Curve Models," Powder Technology, vol. 383, p. 522-535, May 2021.

[9] P. Fu, et al., "Fine Particle Sorting and Classification in the Cyclonic Centrifugal Field," Separation and Purification Technology, vol. 158, pp. 357-366, January 2016.

[10] H. Li, et al., "Operational Performance Characteristics of an Axial Double Baffles Three Channels Classifier for Coarse Pulverized Coal," Powder Technology, vol. 400, Article no. 117250, March 2022.

[11] Z. Sun, et al., "CFD Simulation and Performance Optimization of a New Horizontal Turbo Air Classifier," Advanced Powder Technology, vol. 32, no. 4, pp. 977-986, April 2021.

[12] Z. Sun, et al., "CFD Simulation and Optimization of the Flow Field in Horizontal Turbo Air Classifiers," Advanced Powder Technology, vol. 28, no. 6, pp. 1474-1485, June 2017.

[13] Z. Sun, et al., "Effects of Fine Particle Outlet on Performance and Flow Field of a Centrifugal Air Classifier," Chemical Engineering Research and Design, vol. 117, pp. 139-148, January 2017.

[14] L. Gao, et al., "Study on the Cut Size of a Turbo Air Classifier," Powder Technology, vol. 237, pp. 520-528, March 2013.

[15] R. Liu, et al., "Effects of Axial Inclined Guide Vanes on a Turbo Air Classifier," Powder Technology, vol. 280, pp. 1-9, August 2015.

[16] Y. Yu, et al., "A New Volute Design Method for the Turbo Air Classifier," Powder Technology, vol. 348, pp. 65-69, April 2019.

[17] Q. Huang, et al., "Turbo Air Classifier Guide Vane Improvement and Inner Flow Field Numerical Simulation," Powder Technology, vol. 226, pp. 10-15, August 2012.

[18] Z. Sun, et al., "Structural Optimization of Vortex Finder for a Centrifugal Air Classifier," Chemical Engineering Research and Design, vol. 166, pp. 220-226, February 2021.

[19] M. Betz, et al., "Effects of Flow Baffles on Flow Profile, Pressure Drop and Classification Performance in Classifiers," Processes, vol. 9, no. 7, Article no. 1213, July 2021.

[20] H. A. Petit, et al., "Modelling and Optimization of an Inclined Plane Classifier Using CFD-DPM and the Taguchi Method," Applied Mathematical Modelling, vol. 77, pp. 617-634, January 2020.

[21] M. Barimani, et al., "Particulate Concentration Distribution in Centrifugal Air Classifiers," Minerals Engineering, vol. 126, pp. 44-51, September 2018.

[22] O. Altun, et al., "Selection and Mathematical Modelling of High Efficiency Air Classifiers," Powder Technology, vol. 264, pp. 1-8, September 2014.

[23] T. Yamamoto, et al., "Effect of Inner Structure of Centrifugal Separator on Particle Classification Performance," Powder Technology, vol. 192, no. 3, pp. 268-272, June 2009.

[24] L. Feng, et al., "Classification Performance of Model Coal Mill Classifiers with Swirling and Non-Swirling Inlets," Chinese Journal of Chemical Engineering, vol. 28, no. 3, pp. 777-784, March 2020.

[25] Z. Sun, et al., "Experimental and CFD Study on a Cyclonic Classifier with New Flow Pattern," Advanced Powder Technology, vol. 30, no. 10, pp. 2276-2284, October 2019.

[26] R. Guizani, et al., "Effects of the Geometry of Fine Powder Outlet on Pressure Drop and Separation Performances for Dynamic Separators," Powder Technology, vol. 314, pp. 599-607, June 2017.

[27] K. Elsayed, et al., "Optimization of the Cyclone Separator Geometry for Minimum Pressure Drop Using Mathematical Models and CFD Simulations," Chemical Engineering Science, vol. 65, no. 22, pp. 6048-6058, November 2010.

[28] X. Mou, et al., "CFD-Based Structural Optimization of Rotor Cage for High-Efficiency Rotor Classifier," Processes, vol. 9, no. 7, Article no. 1148, June 2021.

[29] Z. Sun, et al., "A New Static Cyclonic Classifier: Flow Characteristics, Performance Evaluation and Industrial Applications," Chemical Engineering Research and Design, vol. 145, pp. 141-149, May 2019.